

Development of Robust HTS-SQUID for Non-destructive Inspection System in Unshielded Environment

K Yoshida¹, T Kage¹, T. Suzuki¹, Y Hatsukade¹ and S Tanaka¹

¹Toyohashi University of Technology, 1-1 Hibarigaoka, Tempaku-cho, Toyohashi, Aichi 441-8580, Japan

E-mail: hatsukade@ens.tut.ac.jp

Abstract. Cross-shaped $\text{YBa}_2\text{Cu}_3\text{O}_{7-x}$ (YBCO) film was overlapped on directly-coupled multi-pickup-coil HTS-dc-SQUID magnetometer in flip-chip configuration as a superconducting shield, and the characteristics of the SQUID were examined in DC and AC magnetic fields. We created slots in the YBCO film and pickup-coil of HTS-SQUID magnetometer for suppression of flux trapping. In low magnetic field environment, we measured the characteristics of the SQUID without and with HTS film. The most of the parameters were same with and without the HTS films, while $S_\phi^{1/2}$ with the HTS film was a bit smaller than that of the bare SQUID. In the DC field, I_c of the HTS-SQUID covered with the HTS film did not change until a DC field over 140 μT was applied to the SQUID, while the bare SQUID's I_c decreased with the increase of the applied DC field. In the AC fields at 10 MHz, the SQUID with the HTS film showed degradation of the parameters such as V_{pp} and $S_\phi^{1/2}$ at lower field amplitude than the bare SQUID.

1. Introduction

High temperature superconducting (HTS) superconducting quantum interference devices (SQUIDs) have very high magnetic field sensitivity and wide frequency range. Bicrystal grain boundary SrTiO_3 (STO) substrates are commonly used for the HTS-SQUIDs [1]. Fabrication process of single-layer HTS-SQUID based on the bicrystal STO substrates is simple, and offers relatively good characteristics [2]. Therefore, HTS-SQUIDs with bicrystal Josephson junctions have been widely utilized in many field of such as non-destructive inspection (NDI), magnetocardiogram (MCG), geophysical exploration and nuclear magnetic resonance (NMR)/magnetic resonance imaging (MRI) [3-6]. Most of the applications using the HTS-SQUIDs are generally conducted in magnetic shield. However, it is desirable that no magnetic shields are used for practical use. When a conventional bicrystal STO based HTS-SQUID is cooled in an unshielded environment, flux trapping occurs to increase SQUID's noise [7]. In the applications such as NDI, when a bicrystal STO based HTS-SQUID is moved in environmental magnetic field, critical current I_c of the SQUID changes due to the Earth's field (about 50 μT), and flux locked loop circuit cannot keep locking [8]. Therefore, it is difficult to operate the bicrystal STO based HTS-SQUIDs stably and with low noise for such advanced NDI application in the Earth's field [9]. In order to solve these problems, we developed bicrystal STO based HTS-SQUID that can be cooled, operated and moved in unshielded environment for the NDI application.



2. Design of HTS-SQUID magnetometer and HTS film

We designed a directly-coupled HTS-SQUID magnetometer based on a bicrystal STO substrate with misorientation angle of 30 degrees and $\text{YBa}_2\text{Cu}_3\text{O}_{7-x}$ (YBCO) thin film of about 200 nm in thickness. For suppression of the change of critical current I_c by moving a HTS-SQUID in the Earth's field, we designed another HTS film that covered on the SQUID's Josephson junctions. Figure 1 (a) shows design of the directly-coupled HTS-dc-SQUID magnetometer. This SQUID magnetometer had no grain boundary in the pickup-coil because the SQUID had multi-pickup-coil. The SQUID ring is located in the center of the device, and is coupled with the quadruple pickup-coil. The SQUID ring inductance was estimated to be about 52 pH. The pickup-coil of the SQUID was slotted so that the minimum width in the pickup-coil became 5 μm for suppression of flux trapping in cooling in the Earth's field (see Figure 1(c)) [7]. Figure 1(b) shows a pattern of the HTS film. The shape of the HTS film was a cross-shape and had slots such as Figure 1(c). For comparison, we prepared a normal HTS film without slots. The HTS films were designed to cover the SQUID ring and apertures between the pickup-coil. Using the conventional sputtering method, 200 nm-thick YBCO film, for the SQUID and the HTS film, were deposited on the bicrystal and normal STO substrates, respectively. For suppression of the change of I_c , these HTS films were overlapped on the SQUID in flip-chip configuration in experiments in section 3. The position of the HTS films are indicated in Figure 1(a).

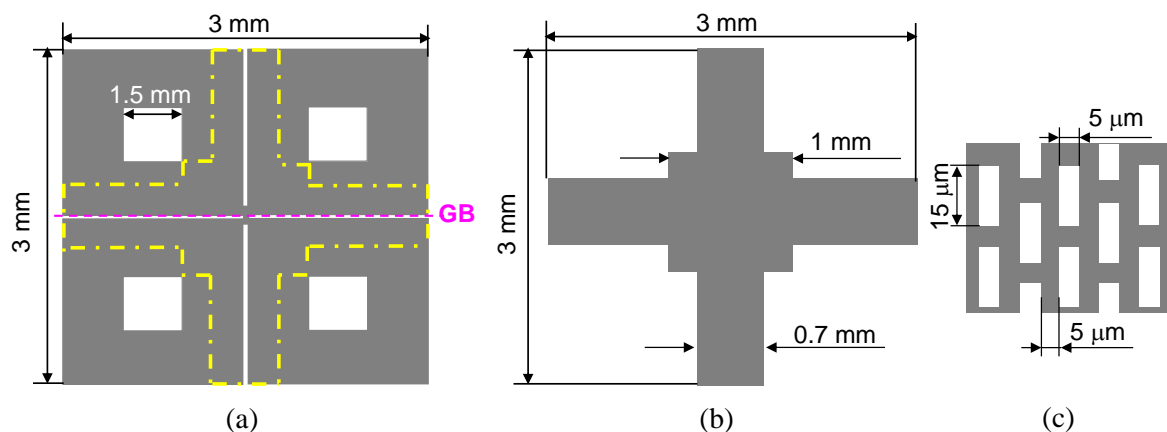


Figure 1. Directly-coupled HTS-dc-SQUID magnetometer with quadruple square pickup-coil. (a) Whole design. Bold chain line indicates the position where the HTS film is overlapped in flip-chip configuration. (b) HTS film. (c) Slots in pickup-coil and HTS film.

3. Experimental Setup

At first, to measure the characteristics of the bare HTS-SQUID magnetometer in a low magnetic field, we set up low field environment in a tri-layer μ -metal shielding case that was set in a moderate magnetically shielded room (MSR). The residual DC field in the case was about 50 nT. We filled liquid nitrogen in a Dewar in the shielding case, and cooled the SQUID in this environment. We measured the characteristics of the bare SQUID such as critical current I_c , normal resistance R_n , modulation voltage V_{pp} and flux noise $S_\phi^{1/2}$. Most of them were measured using a commercial SQUID (Star Cryoelectronics PCI-100) with dc current bias. As shown in the Figure 2(a), to measure the changes in the characteristics of the SQUID in DC field, we applied an DC field from 1 to 500 μT .

Next, for insulation and adhesion, we painted Apiezon grease between the magnetometer and the film in the flip-chip configuration, and pressed them so that the distance between both films became as close as possible. Figure 2(b) shows that the magnetometer and film were tightly connected using polymer threads for reinforcement. The same characteristics of the SQUID magnetometer with HTS film were measured in the same way as above-mentioned. We measured V_{pp} and $S_\phi^{1/2}$ of the uncovered SQUID and the covered SQUID with the HTS films in an AC field at 10 MHz.

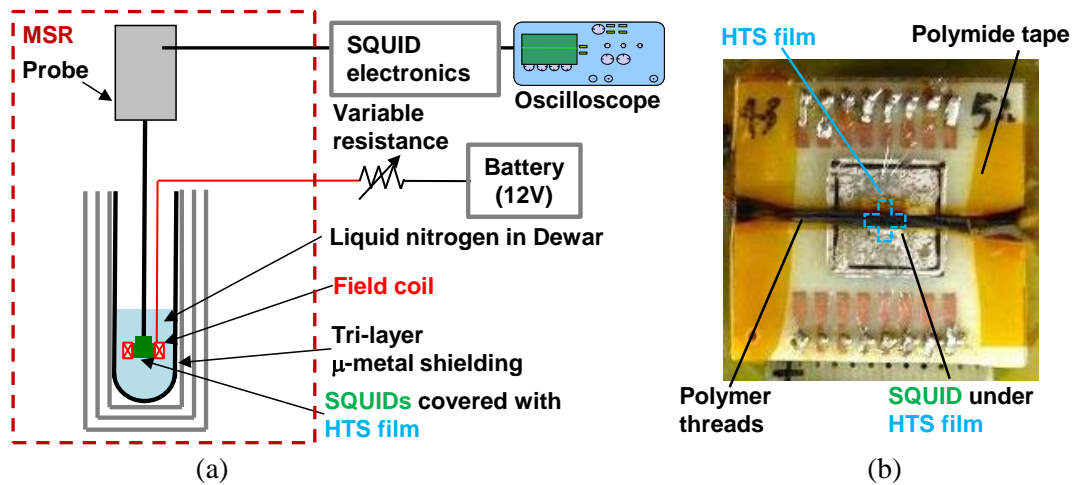


Figure 2. Experimental setup. (a) Measurement setup for SQUID characteristics in moderate MSR. (b) Photograph of HTS-SQUID and HTS film in flip-chip configuration.

4. Results and Discussions

The V - I characteristics, V - Φ characteristics, and flux noise spectra of the HTS-SQUID magnetometer without and with the HTS films in a low magnetic field are summarized in Table 1. I_c , R_n , V_{pp} of the SQUID without and with the HTS films were roughly the same. As shown in the Table 1 and Figure 3, $S_\phi^{1/2}$ decreased a bit with the HTS films on the SQUID. Figure 4 shows the change of I_c when a DC field from 1 to 500 μT was applied to the SQUID. As the DC field increased, I_c of the SQUID without the HTS film immediately decreased. On the other hand, in the case of the SQUID covered with the normal HTS film, the SQUID's I_c did not change until a DC field over 140 μT was applied. It is thought that the HTS film protected the Josephson junctions from DC field. I_c of the SQUID with slot HTS film also did not change until DC field of 140 μT was applied. In comparison with I_c of the SQUID covered with the normal HTS film, I_c of the SQUID covered with slot HTS film decreased gently with the increase of the DC field. Figure 5(a) shows change of V_{pp} when an AC field at 10 MHz was applied to the SQUID with and without the films. When AC field more than 200 nT_{rms} was applied to the SQUID without the HTS film, V_{pp} of the SQUID started to decrease. In contrast, when AC field more than 120 nT_{rms} was applied to the SQUID with the HTS films, SQUID's V_{pp} started to decrease. Figure 5(b) shows change of $S_\phi^{1/2}$ when the AC field was applied. The tendency of the change of $S_\phi^{1/2}$ has similar with those of V_{pp} in Figure 5(a). $S_\phi^{1/2}$ started to increase at 200 nT_{rms} without HTS film, while it started to increase at 120 nT_{rms} with the HTS films.

Table 1. Characteristics of HTS-SQUID without and with HTS films.

Parameter	Without HTS film	With normal HTS film	With slot HTS film
I_c	80 μA	81 μA	80 μA
R_n	1.4 Ω	1.2 Ω	1.3 Ω
V_{pp}	10.7 μV	10.5 μV	10.3 μV
$S_\phi^{1/2}$	50 $\mu\phi_0/\text{Hz}^{1/2}$	35 $\mu\phi_0/\text{Hz}^{1/2}$	45 $\mu\phi_0/\text{Hz}^{1/2}$

5. Conclusions

We overlapped the slot or normal HTS film on the multi-pickup-coil HTS-dc-SQUID magnetometer with slots in the flip-chip configuration. The critical current I_c of the SQUID did not change until a DC field over 140 μT was applied to the SQUID. When an AC field at 10 MHz was applied to the SQUID, V_{pp} of the SQUID decreased and $S_\phi^{1/2}$ increased significantly when the amplitude of the AC field was

about 120 nT_{rms}. The AC field applied to the SQUID at that time was less than that of the bare SQUID. Finally, the experimental results demonstrate that the bicrystal STO based HTS-SQUID covered with the HTS film can be operated and moved in the Earth's field. Further experiments are currently in progress aiming to better understand the reproducibility of the results.

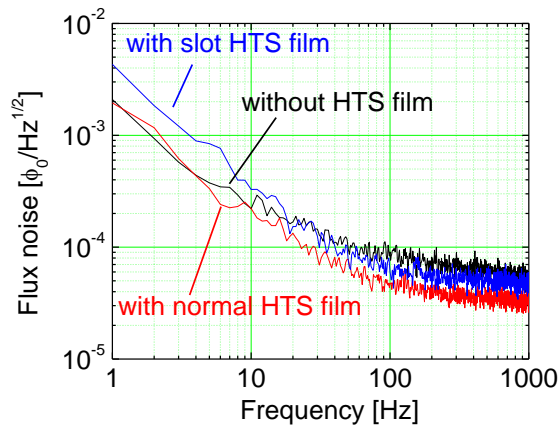


Figure 3. Flux noise spectra of HTS-SQUID without and with HTS films in MSR.

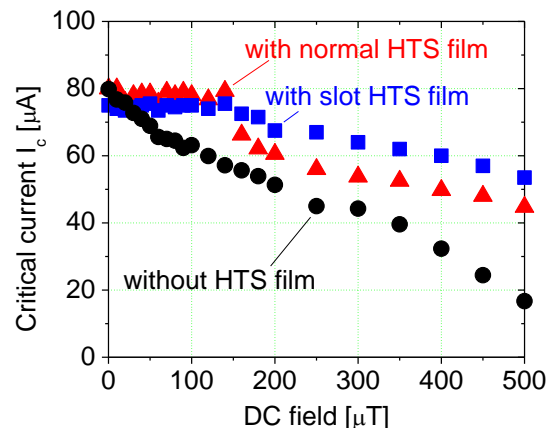


Figure 4. Critical current I_c of HTS-SQUID without and with HTS films in DC field.

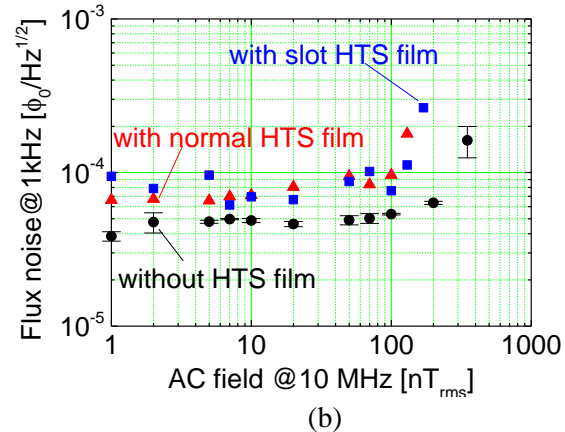
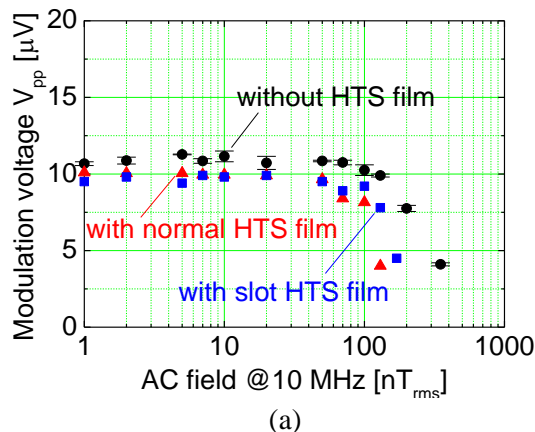


Figure 5. Characteristics of HTS-SQUID without and with HTS films in AC field at 10 MHz. (a) Modulation voltage V_{pp} . (b) Flux noise $S_\phi^{1/2}$ at 1 kHz.

References

- [1] Dimos D, Chaudhari P and Mannhart J 1990 *Phys. Rev. B* **41** 4038
- [2] Clarke J and Braginski A I (ed.) 2004 *The SQUID Handbook*, (Weinheim: WILEY-VCH)
- [3] Barone A (ed.) 1992 *Principles and Application of Superconducting Quantum Interference Device* (Singapore: World Scientific)
- [4] Kobayashi T, Hayakawa H and Tonouchi M (ed.) 2003 *Vortex Electronics and SQUIDs* (Berlin: Springer)
- [5] Kreuzbruck MV, Baby U, Theiss A, Mueck M and Heiden C 1999 *IEEE Trans. Appl. Supercond.* **8** 3805
- [6] Hatsukade Y, Shinyama Y, Yoshida K, Takai Y, Aly-Hassan M S, Nakai A, Hamada H, Adachi S, Tanabe K and Tanaka S 2013 *Physica C* **484** 195
- [7] Dantsker E, Tanaka S, Nilsson P-A, Kleiner R and Clarke J 1996 *Appl. Phys. Lett.* **69** 4099
- [8] Hatsukade Y, Hayashi K, Takemoto M and Tanaka S 2009 *Supercond. Sci. Technol.* **20** S385
- [9] Hatsukade Y, Hayashi K, Shinyama Y, Adachi S, Tanabe K and Tanaka S 2011 *Physica C* **471** 1228